Deep–Sea Research II xxx (xxxx) xxx

Contents lists available at ScienceDirect

Deep-Sea Research Part II

journal homepage: http://www.elsevier.com/locate/dsr2

Deep-sea benthic foraminifera record of the last 1500 years in the North Aegean Trough (northeastern Mediterranean): A paleoclimatic reconstruction scenario

M.D. Dimiza [a], M. Fatourou [a], A. Arabas [b], I. Panagiotopoulos [a,c], A. Gogou [c], K. Kouli [a], C. Parinos [c], G. Rousakis [c], M.V. Triantaphyllou [a,*]

[a] National and Kapodistrian University of Athens, Faculty of Geology and Geoenvironment, Panepistimioupolis, 15784, Athens, Greece
[b] Institute of Geological Sciences, Polish Academy of Sciences, Research Centre in Kraków, ul. Senacka 1, Kraków, 31-002, Poland
[c] Hellenic Centre for Marine Research, Institute of Oceanography, P.O. Box 712, 19013, Anavyssos, Greece

ARTICLE INFO

Keywords:
Benthic foraminifera variation
Organic matter fluxes
Major climatic events

ABSTRACT

A 1500-year, high-resolution deep-sea benthic foraminifera record from the Athos Basin of the North Aegean Trough (northeastern Mediterranean) has been analyzed for the development of a paleoclimatic scenario. The data analysis points out that the quantity and quality of the seafloor's organic matter could be a crucial controlling factor for the faunal succession. During 550–1000 AD (within the Medieval Climate Anomaly), the relatively high benthic foraminiferal accumulation rates together with the predominance of meso-eutrophic taxa, such as *Bolivina dilatata/spathulata*, may be interpreted as the result of high precipitation. Consequently, increased riverine discharges into the North Aegean Sea and the associated warm climatic conditions appear to persist for a long time and are related to a negative phase of the North Atlantic Oscillation. Later on, the establishment of an oligo-mesotrophic seafloor environment is documented by the diminishing benthic foraminiferal accumulation rates associated with an increment in the abundances of *Gyroidinoides altiformis*. During a colder phase of the Little Ice Age (17th century), the relative abundances of the opportunistic foraminiferal species *Bulimina inflata* and *Bulimina marginata* can be related to high marine productivity, most probably due to enhanced winter mixing conditions. Finally, during the last 100 years, a faunal shift to eutrophication preferent species, and the persistent occurrence of *Chilostomella mediterranensis*, reflects a pronounced change in trophic conditions, characterized by high amounts of potentially low-quality organic matter in the seafloor, which are the result of a gradual temperature increase accompanied with enhanced terrigenous inputs.

1. Introduction

High-resolution and well-preserved Holocene sedimentary archives provide climate information on multiple timescales that may contribute to a better understanding of climate sensitivity to internal variability (e.g., atmosphere-ocean feedbacks like the North Atlantic Oscillation – NAO and Atlantic Multi-decadal Oscillation - AMO) and external forcing such as solar radiation and volcanic activity (e.g., Bond et al., 2001; Mayewski et al., 2004; Mann et al., 2009). Recently, an increasing number of studies have interpreted such sedimentary archives from several deep sites in the Mediterranean, offering good evidence of the marine environment responses to the last millennia climate oscillations (Incarbona et al., 2008, 2010; 2016; Piva et al., 2008; Sprovieri et al., 2010; Nieto-Moreno et al., 2011, 2013; Schilman et al., 2011; Grauel et al., 2013; Lirer et al., 2014; Goudeau et al., 2015; Cisneros et al., 2016; Gogou et al., 2016; Margaritelli et al., 2016; Menke et al., 2017). All studies mentioned above report the alternation of decennial to multi-centennial timescale warm and cold events, such as the Medieval Climate Anomaly (MCA: 600–1200 AD), the Little Ice Age (LIA: 1200–1850 AD) and the relatively recent Instrumental Period (IP: 1850 to present). However, the climate responses to these extraordinary events differ temporally among the various Mediterranean sub-basins, presumably affected by the regional and/or large-scale thermohaline/atmospheric circulation patterns (e.g., Gogou et al., 2016).

The Mediterranean climate is influenced by a variety of teleconnection forcing such as NAO, AMO, South Asian Monsoon, Siberian

* Corresponding author.
E-mail address: mtriant@geol.uoa.gr (M.V. Triantaphyllou).

https://doi.org/10.1016/j.dsr2.2019.104705
Received 26 January 2019; Received in revised form 20 September 2019; Accepted 27 November 2019
Available online 29 November 2019

High-Pressure System and El Niño-Southern Oscillation (e.g., Luterbacher and Xoplaki, 2003; Malanotte-Rizzoli et al., 2014). The Aegean Sea, situated in the northeasternmost part of the Eastern Mediterranean, is highly sensitive to recent and past climate fluctuations due to its transitional location between subtropical and temperate climate systems, semi-enclosed nature, small size and complex bathymetry as well as due to the abundance of local freshwater inputs (e.g., Rohling et al., 2002; Ehrmann et al., 2007; Gogou et al., 2007; Kuhnt et al., 2007). The North Aegean Sea is considered an occasional source of deep water formation (a water circulation phenomenon known as the Eastern Mediterranean Transient - EMT), which overflows and spills into the Eastern Mediterranean through the western and eastern Cretan straits (e.g., Theocharis and Georgopoulos, 1993; Roether et al., 1996; Tripsanas et al., 2016). EMT is a result of the strong atmospheric influences during cool and dry winter periods combined with internal thermohaline variability (Zervakis et al., 2000, 2004; Velaoras and Lascaratos, 2010; Androulidakis et al., 2012; Velaoras et al., 2013; Vervatis et al., 2013). The newly-formed dense water is an important source for the ventilation and nutrient regeneration of the deep water layers, especially in the various basins of the North Aegean Sea (Souvermezoglou and Krasakopoulou, 2002). The Aegean Sea, therefore, provides an ideal setting for the investigation of the prevailing surface environmental conditions and vertical fluxes of energy and matter into the deep-water ecosystems.

Benthic foraminifera have been proved to be valuable paleoceanographic and paleoenvironmental proxies since they are an important component of the deep-sea fauna, very susceptible to the recent and past bottom water mass changes (e.g., Gooday et al., 1992). Their distribution and microhabitat structure, as well as the abundances of certain species, are closely related to the quality, quantity and periodicity of the organic matter settling from the surface waters to the seabed as well as the oxygen content of the bottom water layers (e.g., Jorissen et al., 1995, 2007; De Stigter et al., 1998; De Rijk et al., 1999, 2000; Schmiedl et al., 2000; Fontanier et al., 2002). In the oligotrophic deep marine environments, such as these of the modern Mediterranean Sea, which are commonly characterized by good oxygenation, oxygen appears to be a less limiting environmental factor than the sustainable flux of metabolizable organic matter for the distributional patterns and microhabitat depth of most foraminifera species (Jorissen et al., 1995). Therefore, the foraminifera fauna in the extremely oligotrophic deep settings of the Eastern Mediterranean is characterized by low diversity, consisting of typical species with low food demands like *Gyroidina orbicularis*, *Gyroidinoides altiformis* and *Glomospira charoides* (De Rijk et al., 1999; 2000). However, in the North Aegean basins, which are strongly affected by riverine freshwater inputs from the northern borderlands and the Black Sea inflows, the enhanced organic flux into the seafloor causes an increasing contribution of the deep infaunal taxa *Globobulimina* spp., *Chilostomella* spp. and *Bolivina alata* to the foraminifera fauna (Parker, 1958; De Rijk et al., 1999). Besides the investigation concerning the modern benthic foraminifera, the Holocene faunal succession in the different Aegean Sea basins has been widely used for establishing environmental and climatic reconstructions, providing essential information about the response of benthic assemblages to oxygen depletion and/or re-oxygenation during and after sapropel S1 deposition (Geraga et al., 2000; Mercone et al., 2001; Casford et al., 2003; Kuhnt et al., 2007; Abu-Zied et al., 2008; Schmiedl et al., 2010; Triantaphyllou et al., 2016).

The current study presents a 1500-year, high-resolution deep-sea benthic foraminifera record from the Athos Basin (M2 core; North Aegean Trough, northeastern Mediterranean) with the aim to investigate the regional impacts of the recent past climate variability on the North Aegean deep-water ecosystems. The fluctuations in the foraminiferal assemblage density, species composition and diversity parameters were used to reconstruct the status of the bottom water masses and evaluate, for the first time, their response to prevailing paleoenvironmental and paleoclimatic conditions during the latest Holocene. The interpretation of the foraminiferal faunal succession was accomplished taking into account the sea surface salinity (SSS) reconstructions based on planktonic foraminifer *Globigerinoides ruber* (white) oxygen isotope ($\delta^{18}O$) data, alkenone paleothermometry, determinations of organic carbon contents, as well as the $\delta^{13}C_{org}$ and $\delta^{15}N$ data. The findings of this investigation are expected to be considered for comparison purposes by future foraminiferal studies in other deep sites of the Eastern Mediterranean.

2. Regional climate and oceanographic setting

The North Aegean is a continental marginal sea that connects the Eastern Mediterranean with the Black Sea Basin through the Dardanelles and Bosporus straits (Fig. 1A). The North Aegean bottom topography is complex, demonstrating several deep basins and trenches. One of them is the Athos Basin (maximum water depth ~1150 m), which is part of the North Aegean Trough (NAT) that is the most prominent tectonic feature of the North Aegean Sea. The NAT extends NE-SW and consists of the Limnos Basin in the east and the Athos–Sporades Basin in the west (Fig. 1B). Southern, it is separated from the northern Skyros and Chios basins by a sill occurring at ~350 m water depth. The area is influenced by freshwater discharges from major rivers such as Evros, Nestos and Strymon, which drain the north Hellenic borderland and the eastern Turkish coastline (Karamenderes).

In the North Aegean, a Mediterranean-type climate prevails, demonstrating warm-hot dry summers and mild-cold more humid winters (e.g., Poulos et al., 1997). During winter, intense dry and cold polar/continental or arctic air masses from the Balkan Peninsula affect the Aegean evaporation and sea surface temperature (e.g., Theocharis and Georgopoulos, 1993; Poulos et al., 1997; Rohling et al., 2002). The Etesians, which represent a monsoonal-type, cool and dry northeasterly wind system, are active during summer and early autumn being a major climatic element (e.g., Tyrlis et al., 2012).

The hydrographic regime of the North Aegean is characterized by a seasonal variation in the input rates of the Black Sea Water (BSW), entering through the Dardanelles Strait, a northward flow of warm and saltier Levantine Water (LW) and the aforementioned (see section 1) saline, very dense North Aegean Deep Water (NADW) masses (e.g., Zervakis et al., 2000, 2004; Velaoras and Lascaratos, 2005; Androulidakis et al., 2012). The low-salinity (24–28), cold and nutrient-rich BSW is injected into the North Aegean down to 50 m depth and follows the general cyclonic circulation pattern of the Aegean Sea (Zodiatis, 1994) (Fig. 1B). During winter, BSW fills the upper water layers of the northernmost part of the Aegean Sea before its westward migration. During summer, the strong Etesians blowing over the Aegean region divert the BSW flow to some extent south of the Lemnos Island. BSW creates a strong thermohaline front with the saltier (>39), warmer and well-oxygenated LW, which inflows via the eastern Cretan Strait and is directed northwards along the east margin of the Aegean Sea (Zervakis and Georgopoulos, 1998). Finally, the saline, very dense NADW fills the water column of the North Aegean down to 400 m depth (Zervakis et al., 2000, 2004; Velaoras and Lascaratos, 2005) or even deeper (Tripsanas et al., 2016).

The North Aegean region is oligotrophic, showing an estimated annual primary production of ~30 g C m^{-2} yr^{-1} (Ignatiades et al., 2002). However, during the most productive spring period, especially in its northeastern part that is under the direct influence of the BSW, less oligotrophic conditions with high values of nutrients and phytoplankton biomass can occur (Ignatiades et al., 2002; Siokou-Frangou et al., 2002; Zervoudaki et al., 2007; Lagaria et al., 2017), enhancing the organic matter fluxes into the deep-water benthic ecosystem (Lampadariou and Tselepides, 2006; Lampadariou et al., 2017).

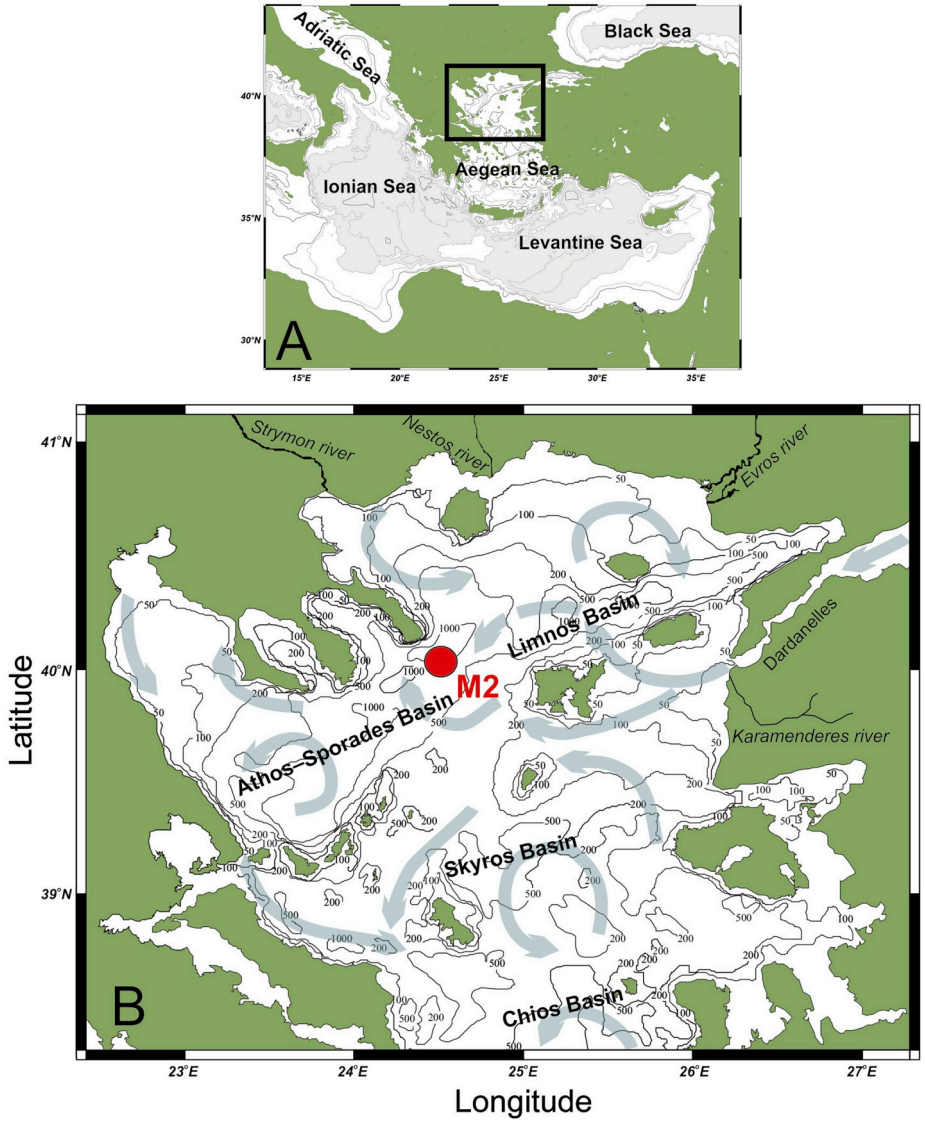

Fig. 1. (A) Location map of the study area in the Eastern Mediterranean. (B) Bathymetric map of the North Aegean Sea showing also the recovery location of the M2 core in the North Aegean Trough. The displayed arrows indicate major circulation patterns of the surface water masses according to Lykousis et al. (2002), Zervakis et al. (2005) and Poulos (2009).

3. Material and methods

3.1. Sedimentary record and age model

The data analyzed for the goals of the current study were obtained from a 48-cm-long sediment core recovered with a multi-corer device, during the 'MEDECOS II' cruise onboard the R/V 'Aegaeo' in 2011, from a water depth of 1018 m (40°05.15′N, 24°32.68′E) in the Athos Basin (see M2 location in Fig. 1B). This core consists of olive grey (2.5GY 5/1; Munsell color chart) to greyish olive (5Y 5/2; Munsell color chart) homogeneous hemipelagic mud with limited sand fractions, less than 5% dw, and silt fractions and $CaCO_3$ contents ranging from 25 to 45% dw and 16–20% dw, respectively (for more details see Roussakis et al., 2004).

The age model of the M2 core was adopted from Gogou et al. (2016), dating back to the last 1500 years. The M2 age control has been accomplished through a combination of ^{210}Pb activity–depth profile and five accelerator mass spectrometry (AMS) ^{14}C dates from planktonic foraminifera tests. The AMS ^{14}C dates have been converted to calendar ages Anno Domini (AD) using the Calib 7.02 software (Reimer et al., 2013) and the MARINE13 calibration dataset, incorporating the correction for the local reservoir effect of $\Delta R = 58 \pm 85$ years (Reimer and McCormac, 2002). Linear interpolation among the ^{14}C dates was applied for the construction of the age-depth profile, with the sedimentation rates showing a progressive decrease from the top to the bottom of the M2 deposit (87-13 cm kyr^{-1}).

Sediment samples, for the subsequent analyses described below, were retrieved from the M2 core at 0.5 cm depth intervals, thus, providing a time resolution of 8–40 years with an average of ~15 years. In this way, a unique, high-resolution sedimentary record for the MCA and LIA events, and IP time span as well (Gogou et al., 2016; Luterbacher et al., 2012) was created.

3.2. Organic carbon, δ^{13}Corg and δ^{15}N of the sediment, and planktonic foraminifera δ^{18}O analyses

96 sediment samples were processed for organic carbon (OC) content determination and δ^{13}Corg analysis, carried out in the University of California, Davis, using a PDZ Europa ANCA-GSL elemental analyser interfaced with a PDZ Europa 20-20 isotope-ratio mass spectrometer. Before the OC determination (precision within 0.02%), the total carbon contents were measured via an OPTIMA isotope-ratio mass

spectrometer, with the analysis precision being ± 0.08%; then the carbonates were removed using 1N hydrochloric acid. The measured $\delta^{13}C_{org}$ values were expressed in ‰ in relation to the standard Vienna Pee Dee Belemnite (VPDB), with the overall analytical error, based on duplicate measurements, estimated at ±0.2‰.

Likewise, ninety-six sediment samples were processed for the total nitrogen (N) content determination and $\delta^{15}N$ analysis, carried out in the University of California, Davis, using an OPTIMA isotope-ratio mass spectrometer interfaced in continuous flow. The measured $\delta^{15}N$ values were expressed in ‰ with the analysis precision estimated ±0.14%.

For the determination of the oxygen isotopic composition ($\delta^{18}O$), thirty-nine sediment samples were used selecting six clean foraminiferal specimens of the planktonic species *Globigerinoides ruber* (white) occurring within the 125–250 μm sediment fraction. The measurements were carried out in the Stable Isotope Laboratory Department of Earth and Planetary Sciences of the University of California, Davis. Repeated measurements performed on triplicates provided standard deviations of ±0.2‰. The $\delta^{18}O$ values were expressed in ‰ in relation to the standard VPDB and were correlated with the available alkenone-derived sea surface temperature (SST) derived for the same sedimentary record (M2) by Gogou et al. (2016).

3.2.1. Sea surface salinity estimation

Salinity changes were calculated using the expression given by Rostek et al. (1993) based on Broecker (1989):

$$S = \Delta S_0 + S^* + (\Delta\delta^{18}O_F - a - b\Delta T)/c, \quad (1)$$

where S and S^* stands for past and present-day local surface salinity, respectively. ΔS_0 express the global change of ocean salinity due to ice shield growth; here treated as 0 due to a short period studied (1500 yrs) when the global ice-volume and ocean salinity did not change remarkably. The correction parameter a stands for the ice volume effect – the time-dependent global variations of seawater $\delta^{18}O$ due to ice shield growth and decay. In the studied period $a = 0$ (Vogelsang, 1990). The constant b relates $\delta^{18}O_{calcite}$ and $\delta^{18}O_{seawater}$ and represents the temperature effect of *G. ruber* on $\delta^{18}O$, which is −0.2‰/K (Duplessy et al., 1981; Emeis et al., 2000). Coefficient c is relating salinity with $\delta^{18}O_{seawater}$. Regarding the young age of the samples, $c = 0.25$‰/p.s.u. as based on a recent extensive survey of the Mediterranean waters that indicate a correspondence between salinity and $\delta^{18}O_{seawater}$ (Pierre, 1999). Finally, ΔT represents the temperature change from modern to past. The alkenone-derived SST values (Gogou et al., 2016) from the core-top were used as our modern end-member to calculate ΔT, what can be a possible source of error in the estimation. This value may not be representative for modern conditions; however, the offset should be systematic, and since relative changes in comparison to current conditions are considered, it should not be of relevance. Another source of error may be a possible seasonal offset in the formation of the isotopic and temperature signal due to the different lifestyles of *G. ruber* and coccolithophore *Emiliania huxleyi* that forms the alkenone signal, since in the method we presumed that their growth season and depth habitats are analogous (compare with Emeis et al., 2000).

3.3. Analysis of benthic foraminiferal assemblages

For benthic foraminiferal analyses, two to 3 g of 95 freeze-dried samples were washed and wet sieved through 63, 125 and 250 μm standard sieves. Sub-samples of >125 μm size were examined under a Leica APO S8 stereoscope, and all benthic specimens were entirely picked, identified and counted (Appendix A-B). Specimens were identified according to the generic classification of Loeblich and Tappan (1987, 1994) and the standardized nomenclature of the World Register of Marine Species (WoRMS, 2018). *Melonis barleeanus* was regarded as a synonym of *Melonis affinis* following the recommendations of Schweizer (2006), while *Bolivina dilatata* and *Bolivina spathulata* were grouped as *Bolivina dilatata/spathulata* due to the presence of transitional forms between these two species.

The number of the benthic foraminifera (BFN) was expressed as specimens per gram of dry bulk sediment for each of the examined samples, whereas the relative abundances (%) for all species were calculated. The benthic foraminiferal accumulation rate (BFAR: number of specimens cm^{-2} kyr^{-1}) was used as a semi-quantitative proxy for the flux of organic carbon into the seafloor (e.g., Jorissen et al., 2007) and was calculated by multiplying the BFN with the dry bulk density (g cm^{-3}) and the linear sedimentation rate (cm kyr^{-1}) (Herguera and Berger, 1991). The foraminiferal species diversity was used to interpret the prevailing environmental conditions. Usually, the benthic foraminiferal fauna in stable, well-oxygenated ecosystems, governed by mesotrophic conditions, are characterized by rich diversity, whereas in ecosystems that exhibit extremely oligotrophic or eutrophic and oxygen-depleted regimes they appear poor diversity featured by the dominance of only a few specific taxa (Jorissen et al., 1995; Schmiedl et al., 1998, 2003). For the aims of this study, the species diversity was estimated by the Shannon–Wiener index: H' = -Σpi x Inpi, where pi is the proportion of each of the species (Shannon and Weaver, 1999), and the exponential form of H', i.e., expH'. The H′ is a measure of heterogeneity evaluation and is based on the distribution of individuals in the different species, while, in contrast, expH′ provides a more realistic representation of the expected species richness in a sediment sample (Jost, 2006). Although the typical of shallow water taxa *Ammonia* spp. and *Elphidium* spp., and epiphytic *Asterigerinata mamilla*, *Planorbulina mediterranensis*, *Neoconorbina terquemi* and *Rosalina* spp. were treated as reworked specimens and excluded from the total sum of the 'intact' benthic foraminiferal (BF) relative abundances, the ratio (%) between the sums of reworked (RW) and total foraminifera (RW + BF) was used as a proxy of matter transport from the inner shelf to the deep-sea environment.

Finally, a Principal Component Analysis (PCA), using the SPSS statistics software (version 21.0), was carried out in order to identify the main components that explain most of the faunal variance (Parker and Arnold, 1999). Only benthic species exceeding relative abundances of 5% in one sediment sample at least were processed for the analysis. The data were logarithmically transformed to reduce the score and bias caused by the more abundant species against the less abundant ones. The Principal Components (PCs) with eigenvalues greater than one were retained (Kaiser, 1960). The environmental variables (alkenone-derived SSTs, OC, C/N and BFAR) were projected on the component plane as additional variables, without contributing to the results of the analysis. This can reveal the potential influence of the environmental parameters on the faunal patterns.

4. Results

4.1. Planktonic foraminifera $\delta^{18}O$ record and organic matter ($\delta^{15}N$, $\delta^{13}Corg$, OC and C/N-ratios) of the sediment

The stable oxygen isotope composition of *G. ruber*, throughout the investigated time interval (500–2003 AD), fluctuates between −0.67 and 1.07‰, displaying an average of 0.32‰. As shown in Fig. 2, a progressive decrease of the $\delta^{18}O_{ruber}$ values between 770 and 1000 AD (reaching a minimum of 0.19‰ in 980 AD) is followed by a rapid increase up to 1‰ in 1165 AD, then a drop to −0.25‰ in 1260 AD and another increase up to 0.8‰ in 1300 AD. Between 1300 and 1470 AD, within the LIA period, the $\delta^{18}O_{ruber}$ values decrease up to −0.3‰ in 1470 AD. Afterwards, until 2003 AD, the $\delta^{18}O_{ruber}$ record is characterized by fluctuations, although the minimum and maximum values of the record appear in this time interval.

For the entire study period, the values of the nitrogen-isotope record range between −3.07 and 5.93‰ (Fig. 2). A decreasing trend is noticed between 500 and 1000 AD (within the MCA period), with values varying from 2.3 to −0.8‰. From 1100 to 1330 AD, the $\delta^{15}N$ values fluctuate

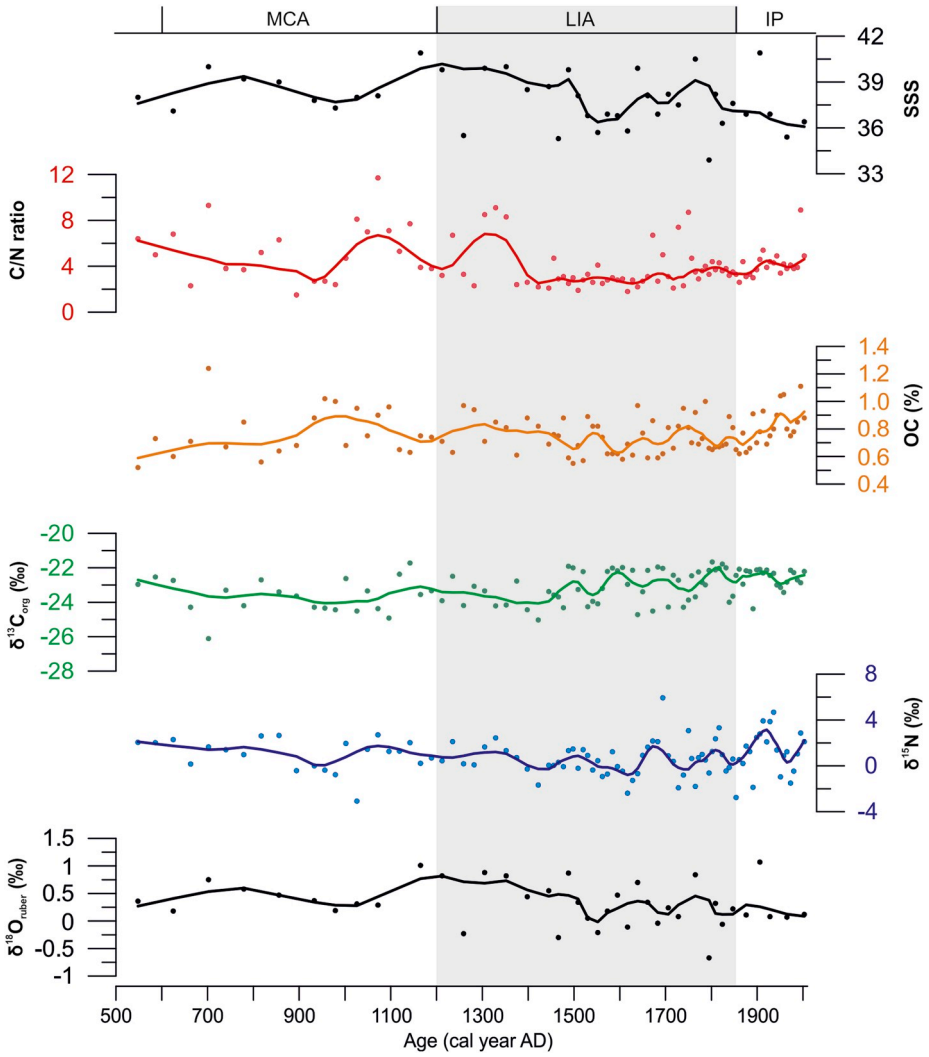

Fig. 2. From bottom to the top: $\delta^{18}O_{ruber}$, $\delta^{15}N$, $\delta^{13}C_{org}$, OC, C/N and SSS profiles derived from the M2 core. All data have been smoothed using a LOESS function (see bold lines).

between 0 and 2.5‰, then decrease to −1.7‰ around 1400 AD and increase again up to 1.5‰ around 1500 AD. Then, the $\delta^{15}N$ values decrease to −2.4‰ in 1620 AD and increase again to 2.1‰ in 1680 AD. After a $\delta^{15}N$ drop to −1.9‰ in 1730 AD, for the next 100 years, the isotopic values vary between −1.8 and 3.3‰. A new $\delta^{15}N$ increase, up to 4.7‰, is observed between 1830 and 1936 AD, followed by a reduction to −1.5‰ in 1973 AD. Finally, during the last decades, the $\delta^{15}N$ record shows an increasing trend reaching a maximum of 2.9‰ around 2000 AD.

The $\delta^{13}C_{org}$ values fluctuate from −26 to −21.7‰ (Fig. 2). Within 500–700 AD, the values decrease from −23 to −26‰, while after a rapid increase in 820 AD (−22.6‰) a new drop to −24.5‰ occurs in 970 AD. Then, a random fluctuation of the record between −22.6 and −25‰ occurs till 1100 AD, when an increase appears in 1140 AD, reaching the peak of the $\delta^{13}C_{org}$ profile. Till 1400 AD, a decline to −25‰ is recorded and since then, till 2003 AD, the $\delta^{13}C_{org}$ values show a variation between −24.7 and −21.7‰ indicating a gradual increasing trend.

During the whole study period, the organic carbon (OC) contents range from 0.52 to 1.24% dw (Fig. 2), with the aforementioned minimum and maximum values appearing within the 500–700 AD interval. A value (0.56% dw) close to the minimum one occurs in 820 AD and since then an increase of the OC content is evident within the MCA period, lasting until 955 AD, with the relevant values reaching up to 1% dw. For the next 300 years, the OC contents gradually decrease to 0.6% dw till 1460 AD, rising again up to 0.97% dw in 1620 AD. Through the next three centuries, the OC contents fluctuate between 0.55 and 1% dw, while an increasing trend (0.6 up to 1.1% dw) is observed during the 1860–2000 AD interval, within the IP period.

The C/N atomic ratio shows one peak (in 1050 AD) towards the end of the MCA period and another one (in 1300 AD) during the commencement of the LIA interval (Fig. 2). However, since then, the C/N values reduce and remain lower during the entire LIA. Afterwards, within the IP period, an increasing trend appears but is characterized by lower values when compared to the MCA interval.

During 600–700 AD, the SSS increases (Fig. 2), while for the next three centuries a decreasing trend is indicated till 1000 AD. Then, towards the end of the MCA period, a significant SSS rise is observed, but after the outset of LIA in 1200 AD, a continuous decline lasting till 1550 AD is noticed. Since then, SSS demonstrates a pronounced fluctuation, which, shows a gradual increase till 1800 AD. Afterwards, during the IP period, SSS consistently reduces displaying lower levels when compared to these associated with the MCA interval.

4.2. *General characteristics of the benthic foraminifera assemblages*

The BFNs of the M2 record range from 24 to 236 sp. g^{-1}, with the average value being 61 sp. g^{-1} (Fig. 3). Two major BFN peaks are observed, a higher between 700 and 800 AD (up to 236 sp. g^{-1}) and a

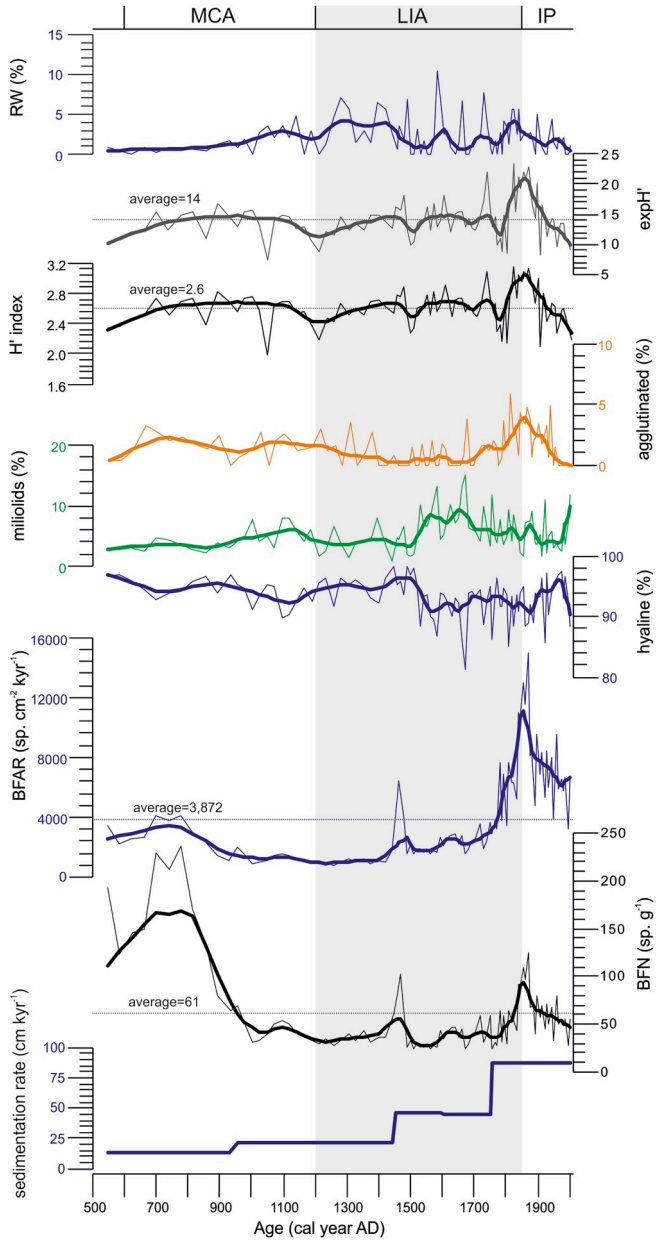

Fig. 3. From bottom to the top: Linear sedimentation rates; Number of benthic foraminifera (BFN); Benthic foraminiferal accumulation rate (BFAR); Relative abundances of calcareous hyaline, porcelaneous (miliolids) and agglutinated tests; Shannon–Wiener index (H′); Exponential form (expH′) of H'; Reworked (RW) specimens in the M2 core. All data have been smoothed using a LOESS function (see bold lines).

lower in the 19th century (up to 126 sp. g^{-1}). However, this is in contrast to the trend illustrated in the BFAR plot (Fig. 3) since the highest peak of the distribution (i.e., ~15,000 sp. cm^{-2} kyr^{-1}) appears in the 19th century; this discrepancy must be the result of the intensification of the sedimentation rate after 1750 AD (Fig. 3). In general, the greater BFAR values (showing an average of ~7500 sp. cm^{-2} kyr^{-1}) are observed from 1800 AD to the present, while the lower ones (showing an average of ~1000 sp. cm^{-2} kyr^{-1}) are noticed within the LIA (between 1200–1400 AD). In addition, secondary BFAR peaks can be seen in 750, 1100, 1450 AD and in the early 17th century, mostly fluctuating below the average (3878 sp. cm^{-2} kyr^{-1}) of the whole record.

Regarding, the foraminifera identification, a total of 142 species (including 96 hyaline, 32 porcellaneous miliolids and 14 agglutinated forms) and 73 genera were recognized (Appendix A). Throughout the studied time interval, the calcareous hyaline taxa appear dominant (85–97%) showing an average relative abundance of 93% (Fig. 3). The miliolids (1.5–12%, average of 5%) show relatively higher relative abundances after 1500 AD, whereas the agglutinated forms (0–6%, average of 2%) display a relatively higher proportion within the 19th century (Fig. 3). The species diversity indices, H′ and expH′, vary from 2.0 to 3.1 (average of 2.6) and from 9 to 23 (average of 14), respectively (Fig. 3) and, in general, both of them show almost identical patterns throughout the entire record. At the beginning of the 19th century, a significant peak in both diversities is detected, which is followed by a progressively decreasing trend during the last 150 years. Finally, the RW values (0–5%, an average of 2%) demonstrate significant fluctuations after 1000 AD (Fig. 3).

4.3. Benthic foraminiferal composition

Eleven hyaline taxa represent 60–90% of all assemblages in the M2 sedimentary record. *Gyroidinoides altiformis*, *Melonis affinis*, *Bolivina dilatata/spathulata*, *Cassidulina carinata*, *Bulimina marginata*, *Cassidulina crassa*, *Uvigerina mediterranea* and *Bulimina inflata* are the most abundant taxa (frequency peaks of >10%), whereas *Uvigerina peregrina*, *Hyalinea balthica* and *Chilostomella mediterranensis* are also well represented (relative abundances of ≥5% in one sample at least). Among miliolids, *Sigmoilopsis schlumbergeri*, *Miliolinella subrotunda*, *Sigmoilinita tenuis* and *Quinqueloculina* spp. are the most common species, while frequently encountered agglutinated foraminifera comprise *Repmanina charoides*, *Spiroplectinella sagittula*, *Siphotextularia concava* and *Textularia* spp.; however, the agglutinated relative abundances do not exceed 5% of the total foraminiferal fauna.

Gyroidinoides altiformis (6–43%, average of 18%) showed relative low abundance (average value of 12%) between 550 and ~1000 AD (Fig. 4). Towards younger ages, the record showed an increasing trend (up to 36% around 1050 AD), with slight fluctuations (average value of 18%). In the second part of the 18th century and early 19th century, the species displayed a significant increase (up to 38%) followed by a marked drop, with a minimum abundance of 8% at 1870 AD. After that, the relative abundance of *G. altiformis* was featured by a rising trend until the present times. The abundance pattern of *M. affinis* (0–38%, averaging 16%) was characterized by a continuous increase from ~700 to ~1450 AD, followed by intense fluctuations within a generally decreasing trend from ~1600 AD to present (Fig. 4). *Uvigerina mediterranea* (0–12%, averaging 5.5%) was slightly enhanced between 1050 AD and 1250 AD; then its abundances displayed significant fluctuations with short lived peaks centred around 1720, 1795 AD and the first half of 20th century. The abundance of *C. crassa* (0–13%, averaging 3.4%) was relatively high from the 1200 AD. *Bolivina dilatata/spathulata* (4–32%, 16% of the assemblages) showed significant abundance throughout the studied interval with maximum increment between 550 and ~1000 AD; its abundance pattern is broadly opposite to that of *G. altiformis* (Fig. 4). *Bulimina marginata* (0–13%, averaging 6%) and *C. carinata* (0–13%, averaging 3.8%) showed more or less similar fluctuations displaying higher percentages until around 1400 AD (Fig. 4). Then, they both decreased until the end of the 16th century; a prominent increase followed until around 1850 AD, after which they showed a subsequent decreasing trend to the top of the record. *Bulimina inflata* (0–11%, averaging 4%) presented notable frequencies between 550 and ~1000 AD, and after 1600 AD until present. The higher frequencies of *U. peregrina* (maximum value 8%) and *H. balthica* (maximum value 5%) occurred since about 1000 AD; both species presented an upward decreasing trend being rare after 1100 AD (Fig. 4). *Chilostomella mediterranensis* (maximum value 5%), being very rare or totally absent since 1900 AD displayed a prominent rise in abundance during the second half of 20th century.

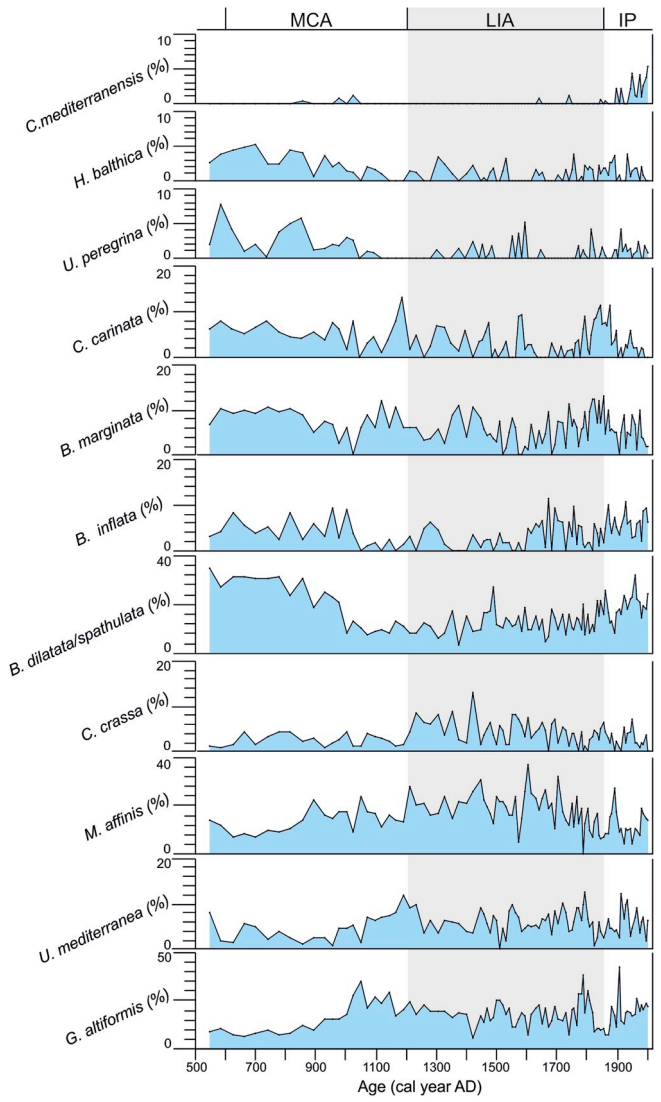

Fig. 4. Relative abundances (%) of the most important species of the benthic foraminifera assemblages in the M2 core.

4.4. Principal Component Analysis

The PCA of the foraminiferal data set enabled an interpretation of the complex patterns of faunal changes in the North Aegean Sea during the past 1500 years. The first three PCs have eigenvalues greater than 1. In this case, the PC1 accounts for 24% of the total variance in the foraminiferal record, while PC2 and PC3 explain a further 16% and 11%, respectively (Table 1).

Table 1
Matrix derived from the Principal Component Analysis. Significant loadings are shown in bold.

	PC1 (24%)	PC2 (16%)	PC3 (11%)
B. dilatata/spathulata	**0.769**	0.265	0.002
B. inflata	0.426	0.301	**0.529**
B. marginata	0.329	−0.410	−0.035
C. carinata	0.491	−0.265	−0.473
C. crassa	−0.153	**−0.569**	0.302
C. mediterranensis	0.221	**0.705**	0.283
G. altiformis	**−0.601**	0.494	−0.191
M. affinis	**−0.535**	−0.334	0.460
U. mediterranea	−0.365	0.179	**−0.560**
U. peregrina	**0.651**	0.060	−0.052
H. balthica	**0.519**	−0.320	−0.076

The 3D component plot (Fig. 5) shows the position of the species in relation to the environmental variables on the first three PCs. *Bolivina dilatata/spathulata*, *U. peregrina* and *H. balthica* have significant positive loadings on the PC1 and appear to follow the increase in BFAR, therefore suggesting an organic flux - dependent effect, while *G. altiformis* and *M. affinis* with negative loadings on the PC1, are negatively correlated with BFAR. *Chilostomella mediterranensis* has a substantial positive contribution to PC2, implying correlation with SSTs and OC. In contrast, *C. crassa* shows significant negative loadings for this component. PC3 is positively loaded mainly by *B. inflata*, with negative loadings for *U. mediterranea*. These species are poorly affected by the studied environmental variables.

According to PC score plots (Fig. 6), positive values of PC1 characterize the periods between 550–1000 AD and 1800 AD-to present, whereas the highest values of PC2 were found after 1900 AD. After 1200 AD, PC3 presents significant fluctuations with a distinct peak of more positive values between 1600 and 1750 AD.

5. Discussion

5.1. Paleoenvironmental interpretation

The benthic foraminiferal assemblage composition in the North Aegean Sea during the past 1500 years, as this is revealed by the analysis of the M2 sedimentary record, is relatively diversified being dominated by typical species of the Mediterranean Sea (e.g., Barmawidjaja et al., 1992; Jorissen, 1987; De Stigter et al., 1998; De Rijk et al., 1999, 2000; Schmiedl et al., 2000). The faunal succession is interpreted in the context of the MCA, LIA and IP paleoclimate phases, using the dating suggested by Luterbacher et al. (2012) and references therein.

5.1.1. Medieval Climate Anomaly (600–1200 AD)

During 550 to ~900 AD, the benthic foraminiferal record is characterized by elevated BFAR (and BFN) values (Fig. 3), suggesting relatively high levels of organic flux into the seabed. This is further supported by the high PC1 score (Fig. 6) associated with a high relative abundance of the *B. dilatata/spathulata* (Fig. 4), which is a taxon

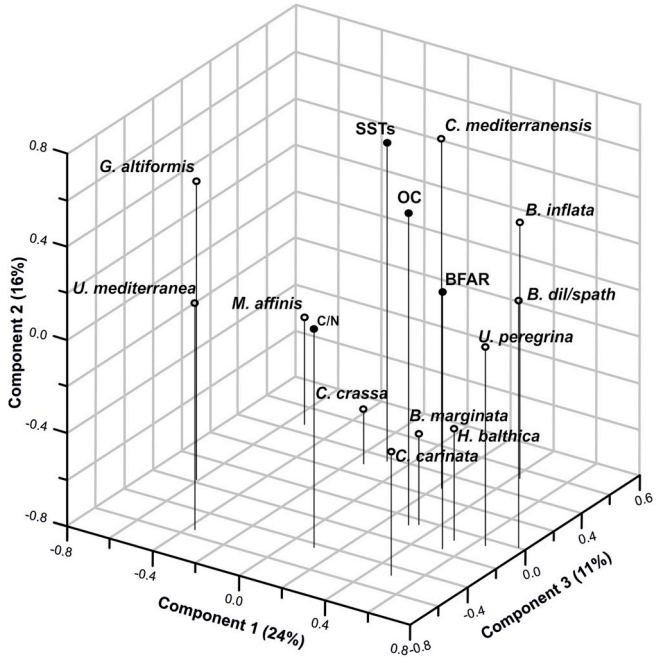

Fig. 5. A PCA-3D plot of the first three principal component axes in Related Space.

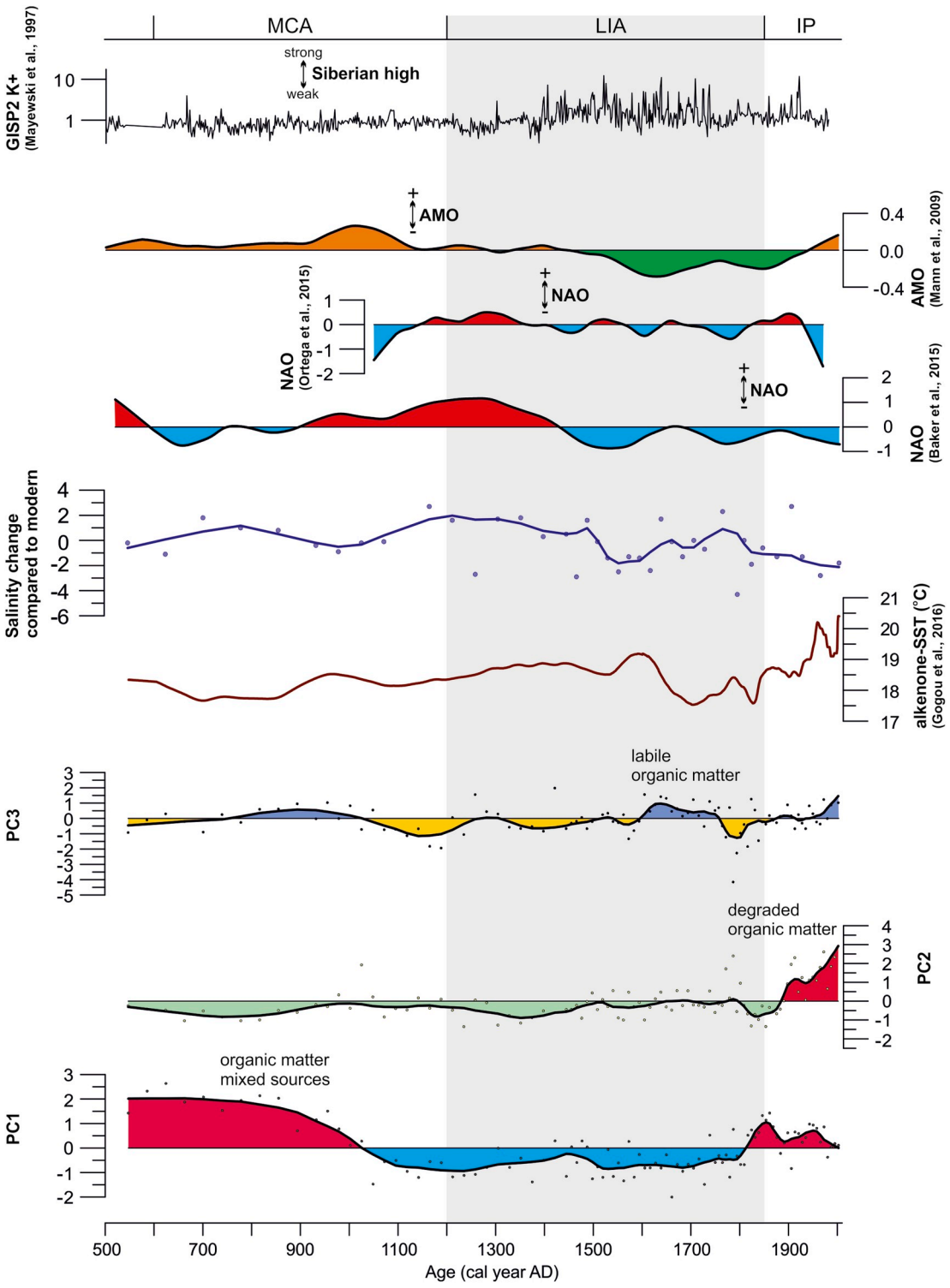

Fig. 6. From bottom to the top: Principal components (i.e., PC1, PC2, PC3) derived from the statistical analysis of the benthic foraminifera assemblages in the M2 core. All data have been smoothed using a LOESS function (see bold lines); Reconstructed changes of salinity (based on the current investigation of the M2 core) compared to the modern one; North Atlantic Oscillation (NAO) index (Baker et al., 2015; Ortega et al., 2015); Atlantic Multidecadal Oscillation (AMO) index (Mann et al., 2009); Siberian high, potassium (K+) content of the Greenland Ice Sheet Project (GISP) 2 ice core (Mayewski et al., 1997).

occupying shallow to intermediate infaunal microhabitats (Barmawidjaja et al., 1992) and considered as an indicator of continuous high organic input (e.g., Barmawidjaja et al., 1992; De Stigter et al., 1998; Mojtahid et al., 2009). Additionally, several epifaunal to shallow infaunal species such as *B. marginata*, *B. inflata*, *C. carinata*, *U. peregrina* and *H. balthica*, which also indicate mesotrophic to eutrophic environment receiving fresh organic matter (e.g., Jorissen, 1987; De Rijk et al., 1999; 2000; Morigi et al., 2001), have a constant presence in the record of this interval (Fig. 4). The dominant *B. dilatata/spathulata* is well known for its tolerance to oxygen-depleted conditions (Jorissen, 1999) that may occur in response to an increase of the organic carbon loading of the sediment. Oxygen consumption due to organic

degradation of labile organic matter and weak ventilation from the overlying water masses can lead to oxygen depletion (Jorissen et al., 1995). Within MCA times, the deep-water formation in the Eastern Mediterranean was probably less than today (Siani et al., 2013), negatively affecting the ventilation of benthic ecosystems. Under such low oxygen conditions, the anaerobic microbial process on organic matter enables nitrate consumption, which is recorded by the decreasing trends of the $\delta^{15}N$ and C/N ratios till 900 AD (Fig. 2). The ^{15}N depletion of the organic substrate seems to be the result of a loss of ^{15}N-enriched nitrogen, due to ^{15}N-ammonia formation by nitrate reduction, which, can produce bacterial biomass characterized by low values of $\delta^{15}N$ and C/N atomic ratio below the oxycline (Libes and Deuser, 1988; Arnaboldi and Meyers, 2006). However, the relatively diversified foraminiferal assemblages, characterized by a typical for marine environment H′ index (2.4–2.8) (Fig. 3), along with the almost absence of more resistant to low-oxygen conditions deep infaunal species, such as *C. mediterranensis*, during this time interval suggest that severe hypoxic conditions were not actually established in the Athos Basin.

Strong indications of gradual enhancement of the trophic conditions are also evident by the OC and $\delta^{13}C_{org}$ curves (Fig. 2). Moreover, the $\delta^{13}C_{org}$ values, as an indicator of the origin of organic matter (marine versus terrestrial), can be used to interpret the role of riverine/continental runoffs. During the whole study period, the $\delta^{13}C_{org}$ values vary mainly between −25‰ and −22‰ indicating a predominance of OC from marine source (Meyers, 1994). Still, the relatively lighter values within the MCA interval, suggest an increased contribution of terrestrial organic carbon to the total organic pool. Indeed, the findings of Gogou et al. (2016) suggest that the higher concentrations of biomarkers together with the depleted $\delta^{13}C_{org}$ values in the M2 deposit prior to 900 AD must be the result of higher precipitation and, consequently, higher contributions from the riverine runoffs to the North Aegean Sea.

Around 1000 AD, a distinct change in the density and the composition of benthic fauna is observed. BFAR and BFN values, generally, exhibit a rapid decrease (Fig. 3). At the same time, *B. dilatata/spathulata* appears significantly reduced reaching a relative abundance about 50% less than the one prior to 1000 AD, while it is accompanied by a contemporaneous prevalence of *G. altiformis* (Fig. 4), which is a shallow infaunal species commonly occurring in mesotrophic to oligotrophic environments (e.g., De Rijk et al., 2000; Abu-Zied et al., 2008). The findings above suggest a reduction of the nutrient influx to the seabed during this time.

Interestingly, slightly increased frequencies of the shallow infaunal taxa *B. marginata* and *U. mediterranea* since the second half of the 11th century (Fig. 4), can imply relatively higher food availability. The latter species is usually common and persistent in the Holocene assemblages of the North Aegean and is generally considered as an indicator of a regular organic supply from the river systems and Black Sea inflows in the area (Schmiedl et al., 2010). Both species are also indicative of well-oxygenated bottom waters (Morigi et al., 2001); an interpretation that is also supported by the increased $\delta^{15}N$ and C/N values (Fig. 2). Under oxic conditions, due to microbial mineralization, the amount of nitrogen in sediments is reduced, and light ^{14}N is preferentially lost from the organic substrate, which becomes progressively enriched in heavy ^{15}N. Therefore, highly decomposed organic matter contains little nitrogen characterized with high C/N ratios and high $\delta^{15}N$ values (e.g., Altabet, 1988; Altabet and François, 1994; Thornton and McManus, 1994).

5.1.2. Little Ice Age (1200–1850 AD)

In the 1200–1450 AD interval, the BFAR and BFN values remain on much lower levels in comparison to those within the MCA period (Fig. 3), and the benthic species diversity (H′ and expH′) shows some decline, reflecting low organic matter flux into the seafloor. Furthermore, PC1 persists in negative scores and only PC3, in certain time intervals, displays eventually not negative or even significant high scores (Fig. 6). Regarding the foraminiferal contents, the strong dominance of *G. altiformis* and intermediate infaunal species *M. affinis* (Fig. 4) supports the interpretation of the occurrence of oligo-mesotrophic conditions with an extensive oxygenated layer at the surface sediment (Abu-Zied et al., 2008). Interestingly, the shallow infaunal species *C. crassa*, which also prefers oligotrophic to mesotrophic environments and indicates a well-ventilated regime (De Rijk et al., 2000), presents a slight increase during the early LIA interval, linked to moderate SST and high SSS values (Figs. 4 and 6). Since 1450 AD, the increasing BFARs associated with the rising relative abundance of *B. dilatata/spathulata* can be attributed to strengthened continental freshwater discharges into the North Aegean, evidenced by lipid biomarker data and a pollen-derived fluvial discharge index (see Gogou et al., 2016). The decreasing salinity further favours this scenario until 1600 AD (Figs. 2 and 6). After 1600 AD, the enhanced marine productivity (Gogou et al., 2016) and associated organic matter fluxes into the deep-water environments can be documented by an increase of the relative abundances of opportunistic taxa such as *B. inflata* and *B. marginata* (see also the PC3 positive scores in Fig. 6). Moreover, salinity increases again, while the gradually elevated $\delta^{15}N$ and C/N ratios imply the establishment of oxic conditions in the area (Fig. 2). Between 1770 and 1820 AD, the important relative frequency peaks of *G. altiformis* and *U. mediterranea* (Fig. 4) suggest a decline of food supply to the sea floor. For the same time interval, a distinct reduction in the riverine discharges into North Aegean is reported by Gogou et al. (2016). Afterwards, a shift to relatively high PC1 scores (Fig. 6) together with (i) a noteworthy rise in BNF, BFAR and diversity indexes (H′ and expH′) (Fig. 3), (ii) a sharp reduction of the *G. altiformis* relative abundance (Fig. 4) and (iii) new peaks in the frequencies of *B. dilatata/spathulata*, *B. marginata* and *C. carinata* (Fig. 4) evidence a more eutrophic marine environment. Additional support for the last interpretation is provided by Skampa et al. (2019) who have reported for the same period in the North Aegean an increase in surface productivity coupled with the dominance of the coccolithophore *E. huxleyi* and a simultaneous lowering of the stratification index coupled with positive NAO shifts. All the aforementioned pieces of evidence could be further connected to the cold event of 1832 ± 15 AD (Gogou et al., 2016), which has been related to volcanic forcing-driven (i.e., the extreme Tambora volcano eruption in 1815 AD; Stothers, 1984) cooling of the global near-surface temperatures within the Dalton solar minimum (1790–1830 AD; e.g., Wagner and Zorita, 2005).

Finally, although the RW profile during LIA (Fig. 3), does not demonstrate significantly high values, its intense fluctuations could reflect sediment transportation due to the relative activity of bottom currents; a prominent increase is noted during the 14th century, while significant peaks are also detected at around 1590, 1730 and 1830 AD. These findings fit nicely to a series of recorded EMT-like events at 1812 ± 18, 1725 ± 25 and 1580 ± 30 AD (Incarbona et al., 2016), which are coupled either with positive NAO shifts and/or reduced solar activity and strong volcanic eruptions.

5.1.3. Instrumental Period (after 1850 AD)

After 1850 AD the benthic foraminiferal assemblage, on average is characterized by increased BFARs, while the diversity decreases continually until the present time (Fig. 3). In-between 1850–1900 AD, *Bolivina dilatata/spathulata* is enhanced and dominates the assemblages; simultaneous low frequencies of *G. altiformis* are documented similarly to those of the early MCA period, however now under lower SSS conditions (Figs. 4 and 6). After 1900 AD, the fauna is characterized by the gradual establishment of the modern foraminiferal assemblage, e.g., *G. altiformis*, which is an important component in the recent oligotrophic environments of the eastern Mediterranean (De Rijk et al., 1999; 2000) presents an increase contrary to the MCA interval, but *B. dilatata/spathulata* still dominates the assemblage. Furthermore, a decrease of *C. carinata* and *B. marginata* and a slight increment of less opportunistic *U. mediterranea* (Fig. 4), suggest the presence of low quality organic fluxes, linked with elevated terrigenous inputs through the northern borderland river systems and the Black Sea inflows

(Schmiedl et al., 2010). High PC3 scores are associated with the appearance of the deep infaunal *C. mediterranensis* (Figs. 4 and 6), which can feed on more degraded organic matter below the sediment-water interface and is well adapted in low oxygen conditions (Fontanier et al., 2002). The degree of organic matter preservation is also reflected in changes in the $\delta^{15}N$, $\delta^{13}C_{org}$ and C/N ratio values (Fig. 2). Evidently, upon degradation of organic matter, C/N ratio increases while $\delta^{13}C$ values slightly decrease (e.g., Ogrinc et al., 2005) and high $\delta^{15}N$ values corresponding with a high C/N ratio suggest diagenesis of the organic matter (e.g., Thornton and McManus, 1994). All evidences suggest a trend towards eutrophicated conditions, feasibly induced by the rising SSTs (Fig. 6) being accompanied by enhanced terrigenous inputs and the concomitant algal productivity in the euphotic zone (Gogou et al., 2016; Skampa et al., 2019).

5.2. A synthesis of the foraminiferal assemblage response to climate variability

The analysis of the deep-water benthic foraminifera succession in North Aegean indicates that an important controlling factor for their abundance and distribution during the last 1500 years could be the quantity and quality of the seafloor's organic matter. Although the late Holocene was mainly characterized by relative low productivity rates and well ventilated conditions (Abu-Zied et al., 2008), time intervals with higher values of BFAR and abundance of more eutrophic foraminiferal species indicate phases with increased organic matter fluxes to the sea floor. Since the fresh marine organic matter (phytodetritus) is the main food source for benthic foraminifera, changes in primary productivity have a strong influence on the densities and composition of assemblages (Fontanier et al., 2006). However, the organic matter in the North Aegean is described as a mixed contribution from autochthonous labile and terrestrial organic matter. The latter, contain more refractory component with a low nutritional value for the benthic foraminifera (e.g., De Rijk et al., 2000).

Based on the PCA, three distinct faunal changes are evidencing the effect of climate variability in the North Aegean ecosystems.

The most prominent faunal change occurs around 1000 AD (see PC1 in Fig. 6), when the oligo-mesotrophic *G. altiformis* replaces the more eutrophic *B. dilatata/spathulata* in the benthic assemblage (Fig. 4). This most probably reflects a response to the modification of the rate of the continental freshwater inputs to the North Aegean Sea as this is further evidenced by the SSS decrement (Figs. 2 and 6). Interestingly, the change mentioned above is climatically related with the shift of NAO to a positive phase ~1000 AD (or even earlier) after a prolonged period of a predominantly negative NAO mode (Fig. 6; Baker et al., 2015). It is well known that NAO is the dominant large-scale climate mode of the wintertime variability in the Northern Hemisphere causing impacts on the temperature and precipitation patterns and, subsequently, on the hydro-climatological characteristics of the Mediterranean Sea (e.g., Luterbacher and Xoplaki, 2003; Brandimarte et al., 2011). In the Aegean Sea, the negative winter NAO phase is connected with a general increase in the precipitation frequency, triggering, consequently, extensive continental runoff. In contrast, the positive NAO phases are often associated with drier conditions as a result of the northward track of the westerlies (e.g., Tsimplis and Rixen, 2002; Brandimarte et al., 2011; Skliris et al., 2012) and a consequent upper water column mixing (Skampa et al., 2019).

After a continuous positive NAO phase until around 1450 AD, a more variable, primarily negative (see curves by Baker et al., 2015 and Ortega et al., 2015 in Fig. 6), affects the benthic fauna record till around 1600 AD, resulting in some recovery of *B. dilatata/spathulata*. At the same time, the AMO is switched into a strongly cooling mode (Mann et al., 2009) (Fig. 6), whereas the accompanied more intense Siberian high contributes to an enhanced invasion of northeasterly cold wind/polar air over the Aegean Sea (Mayewski et al., 1997; Rohling et al., 2002) (Fig. 6), promoting winter mixing conditions and stimulating primary marine productivity (e.g., Skampa et al., 2019) that eventually results in an increased provision of organic matter to the deep benthic ecosystems. Therefore, although the benthic foraminiferal assemblages during the LIA seem to be controlled by relatively oligo-mesotrophic conditions, an increase in the abundance of opportunistic foraminiferal species like *B. inflata* in the 17th century (Fig. 4) supports higher trophic levels (see PC3 in Fig. 6). This shift is potentially strengthened by the substantial decrease in SST (Gogou et al., 2016) (Fig. 6) during the Maunder Minimum (1645–1715 AD) of solar activity and the related SSS increasing trend; this activity could have resulted in deep-water formation events (e.g. Velaoras et al., 2017).

After around 1800 AD, the high sedimentation rates can be mostly associated with the increased terrigenous components from the surrounding borderlands (Roussakis et al., 2004), associated with high precipitation during a predominantly negative NAO mode (Fig. 6) as evidenced by the SSS decrement (Figs. 2 and 6). Simultaneously, they can be linked to the productivity increment as this is evidenced by the highest values of BFAR (Fig. 3). During the 20th century, the benthic faunal shift to more eutrophic content and, especially, the persistent occurrence of *C. mediterranensis* (Fig. 4) reflects a pronounced change in trophic conditions, i.e., higher degradation of the organic matter as a response to the progressive increase in SST (De Rijk et al., 2000) that is clearly indicated in PC2 loading (Fig. 6).

6. Conclusions

Variations in a benthic foraminifera record, obtained from the Athos Basin of the North Aegean (northeastern Mediterranean), of the last 1500 years coincide with distinct shifts in the palaeoenvironmental and climatic changes in the broader area. The replacement of the relatively eutrophic *Bolivina dilatata/spathulata* assemblage by the oligo-mesotrophic *Gyroidinoides altiformis* assemblage after 1000 AD is a response to decreased precipitation and lower contributions from the continental runoff. These conditions are connected to positive NAO phase after an extensive time interval of a dominant negative NAO mode. An increase in the abundance of opportunistic species like *Bulimina inflata* during the 17th century implies relatively higher trophic levels in response to a cooler phase of Little Ice Age. A gradual shift of the benthic fauna to a more eutrophic content, i.e., the appearance of the deep infaunal *Chilostomella mediterranensis*, during the last 100 years, suggests mainly a response to recent warming of the surface waters. Finally, the data analysis indicates that changes in quantity and quality of the sedimentary organic matter is an important controlling factor for the foraminiferal abundance, proving that degraded organic matter are prominently associated with the increment of *C. mediterranensis* within the Instrumental Period.

Acknowledgements

The funding for the fulfilment of the current investigation was provided by the Greek National Project KRIPIS (Integrated Observatories in the Greek Seas - IO, HCMR-MIS 451724; NSRF), the European Research Project MedEcos (MarinERA, EU/FP6) and the IKYDA program of the DAAD (project 57260124 AegeanCocco). We are grateful to two anonymous referees and the journal editor Michele Giani for their valuable input in improving the original manuscript.

Appendix A. Supplementary data

Supplementary data to this article can be found online at https://doi.org/10.1016/j.dsr2.2019.104705.

References

Abu-Zied, R.H., Rohling, E.J., Jorissen, F.J., Fontanier, C., Casford, J.S.L., Cooke, S., 2008. Benthic foraminiferal response to changes in bottom-water oxygenation and

organic carbon flux in the eastern Mediterranean during LGM to Recent times. Mar. Micropaleontol. 67, 46–68.
Altabet, M.A., 1988. Variations in nitrogen isotopic composition between sinking and suspended particles: implications for nitrogen cycling and particle transformation in the open ocean. Deep Sea Res. Part I 35, 535–554.
Altabet, M.A., François, R., 1994. Sedimentary nitrogen isotopic ratio as a recorder for surface ocean nitrate utilization. Glob. Biogeochem. Cycles 8, 103–116.
Androulidakis, Y.S., Kourafalou, V.H., Krestenitis, Y.N., Zervakis, V., 2012. Variability of deep water mass characteristics in the North Aegean Sea: the role of lateral inputs and atmospheric conditions. Deep Sea Res. Part I 67, 55–72.
Arnaboldi, M., Meyers, P.A., 2006. Patterns of organic carbon and nitrogen isotopic compositions of latest Pliocene sapropels from six locations across the Mediterranean Sea. Palaeogeogr. Palaeoclimatol. Palaeoecol. 235, 149–167.
Baker, A., Hellstrom, C., Kelly, B.F.J., Mariethoz, G., Trouet, V., 2015. A composite annual-resolution stalagmite record of North Atlantic climate over the last three millennia. Sci. Rep. 5, 10307.
Barmawidjaja, D.M., Jorissen, F.J., Puskaric, S., Van der Zwaan, G.J., 1992. Microhabitat selection by benthic foraminifera in the northern adriatic sea. J. Foraminifer. Res. 22, 297–317.
Bond, G., Kromer, B., Beer, J., Muscheler, R., Evans, M.N., Showers, W., Hoddmann, S., Lotti-Bond, R., Hajdas, I., Bonani, G., 2001. Persistent solar influence on North Atlantic climate during the holocene. Science 294, 2130–2136.
Brandimarte, L., Di Baldassarre, G., Bruni, G., D'Odorico, P., Montanari, A., 2011. Relation between the north-Atlantic oscillation and hydroclimatic conditions in Mediterranean areas. Water Resour. Manag. 25, 1269–1279.
Broecker, W.S., 1989. The salinity contrast between the Atlantic and Pacific oceans during glacial times. Paleoceanography 4, 207–212.
Casford, J.S.L., Rohling, E.J., Abu-Zied, R.H., Fontanier, C., Jorissen, F.J., Leng, M., Schmiedl, G., Thomson, J., 2003. A dynamic concept for eastern Mediterranean circulation and oxygenation during sapropel formation. Palaeogeogr. Palaeoclimatol. Palaeoecol. 190, 103–119.
Cisneros, M., Cacho, I., Frigola, J., Canals, J.M., Masqué, P., Martrat, B., Casado, M., Grimalt, J.O., Pena, L.D., Margaritelli, G., Lirer, F., 2016. Sea surface temperature variability in the central-western Mediterranean Sea during the last 2700 years: a multi-proxy and multi-record approach. Clim. Past 12, 849–869.
De Rijk, S., Troelstra, S.R., Rohling, E.J., 1999. Benthic foraminiferal distribution in the Mediterranean Sea. J. Foraminifer. Res. 29, 93–103.
De Rijk, S., Jorissen, F.J., Rohling, E.J., Troelstra, S.R., 2000. Organic flux control on bathymetric zonation of Mediterranean benthic foraminifera. Mar. Micropaleontol. 40, 151–166.
De Stigter, H.C., Jorissen, F.J., Van der Zwaan, G.J., 1998. Bathymetric distribution and microhabitat partitioning of live (rose Bengal stained) benthic foraminifera along a shelf to bathyal transect in the southern Adriatic Sea. J. Foraminifer. Res. 28 (1), 40–65.
Duplessy, J.C., Be, A.W.H., Blanc, P.L., 1981. Oxygen and carbon isotopic composition and the biogeographic distribution of planktonic foraminifera in the Indian Ocean. Palaeogeogr. Palaeoclimatol. Palaeoecol. 33, 9–47.
Ehrmann, W., Schmiedl, G., Hamann, Y., Kuhnt, T., Hemleben, C., Siebel, W., 2007. Clay minerals in lateglacial and holocene sediments of the northern and southern Aegean Sea. Palaeogeogr. Palaeoclimatol. Palaeoecol. 249, 36–57.
Emeis, K.C., Sakamoto, T., Wehausen, R., Brumsack, H.J., 2000. The sapropel record of the eastern Mediterranean Sea – results of ocean drilling program leg 160. Palaeogeogr. Palaeoclimatol. Palaeoecol. 158, 371–395.
Fontanier, C., Jorissen, F.J., Licari, L., Alexandre, A., Anschutz, P., Carbonel, P., 2002. Live benthic foraminiferal faunas from the Bay of Biscay: faunal density, composition and microhabitats. Deep-Sea Res. Part I 49, 751–785.
Fontanier, C., Mackensen, A., Jorissen, F.J., Anshutz, P., Licari, L., Griveaud, C., 2006. Stable oxygen and carbon isotopes of live benthic foraminifera from the Bay of Biscay: microhabitat impact and seasonal variability. Mar. Micropaleontol. 58, 159–183.
Geraga, M., Tsaila-Monopolis, S., Ioakim, Chr, Papatheodorou, G., Ferentinos, G., 2000. Evaluation of palaeoenvironmental changes during the last 18,000 years in the Myrtoon basin, SW Aegean Sea. Palaeogeogr. Palaeoclimatol. Palaeoecol. 156, 1–17.
Gogou, A., Bouloubassi, I., Lykousis, V., Arnaboldi, M., Gaitani, P., Meyers, P.A., 2007. Organic geochemical evidence of late glacial-holocene climate instability in the north Aegean sea. Palaeogeogr. Palaeoclimatol. Palaeoecol. 256, 1–20.
Gogou, A., Triantaphyllou, M., Xoplaki, E., Izdebski, A., Parinos, C., Dimiza, M., Bouloubassi, I., Luterbacher, J., Kouli, K., Martrat, B., Toreti, A., Fleitmann, D., Rousakis, G., Kaberi, H., Athanasiou, M., Lykousis, V., 2016. Climate variability and socio-environmental changes in the northern Aegean (NE Mediterranean) during the last 1500 years. Quat. Sci. Rev. 136, 209–228.
Gooday, A.J., Levin, L.A., Linke, P., Heeger, T., 1992. The role of benthic foraminifera in deep-sea food webs and carbon cycling. In: Rowe, G.T., Pariente, V. (Eds.), Deep-sea Food Chains and the Global Carbon Cycle. Kluwer Academic Publishers, Dordecht, pp. 63–91.
Goudeau, M.L.S., Reichart, G.-J., Wit, J.C., de Nooijer, L.J., Grauel, A.-L., Bernasconi, S. M., de Lange, G.J., 2015. Seasonality variations in the central mediterranean during climate change events in the late Holocene. Palaeogeogr. Palaeoclimatol. Palaeoecol. 418, 304–318.
Grauel, A.-L., Goudeau, M.-L.S., de Lange, G.J., Bernasconi, S.M., 2013. Climate of the past 2500 years in the Gulf of Taranto, Central Mediterranean Sea: a high resolution climate reconstruction based on $\delta^{18}O$ and $\delta^{13}C$ of *Globigerinoides ruber* (white). Holocene 23, 1440–1446.
Herguera, J.C., Berger, W.H., 1991. Paleoproductivity from benthic foraminifera abundance: glacial to postglacial change in the west equatorial Pacific. Geology 19, 1173–1176.
Ignatiades, L., Psarra, S., Zervakis, V., Pagou, K., Souvermezoglou, E., Assimakopoulou, G., Gotsis-Skretas, O., 2002. Phytoplankton size-based dynamics in the Aegean Sea (eastern mediterranean). J. Mar. Syst. 36 (1–2), 11–28.
Incarbona, A., Bonomo, S., Di Stefano, E., Zgozi, S., Essarbout, N., Talha, M., Tranchida, G., Bonanno, A., Patti, B., Placenti, F., Buscaino, G., Cuttitta, A., Basilone, G., Bahri, T., Massa, F., Censi, P., Mazzola, S., 2008. Calcareous nannofossil surface sediment assemblages from the Sicily Channel (central Mediterranean Sea): palaeoceanographic implications. Mar. Micropaleontol. 67, 297–309.
Incarbona, A., Di Stefano, E., Sprovieri, R., Bonomo, S., Pelosi, N., Sprovieri, M., 2010. Millennial-scale paleoenvironmental changes in the central Mediterranean during the last interglacial: comparison with European and North Atlantic records. Geobios 43, 111–122.
Incarbona, A., Matrat, B., Mortyn, G.P., Sprovieri, M., Ziver, i P., Gogou, A., Jorda, G., Xoplaki, E., Luterbacher, J., Langone, L., Marino, G., Rodriguez-Sanz, L., Triantaphyllou, M., Di Stefano, E., Grimalt, J.O., Tranchida, G., Spriovieri, R., Mazzola, S., 2016. Mediterranean circulation perturbations over the last five centuries: relevance to past Eastern Mediterranean Transient-type events. Sci. Rep. 6, 29623.
Jorissen, F.J., 1987. The distribution of benthic foraminifera in the Adriatic Sea. Mar. Micropaleontol. 12, 21–48.
Jorissen, F.J., 1999. Benthic foraminiferal microhabitats below the sediment-water interface. In: Sen Gupta, B.K. (Ed.), Modern Foraminifera. Kluwer Academic Publishers, Dordrecht, pp. 161–179.
Jorissen, F.J., De Stigter, H.C., Widmark, J.G.V., 1995. A conceptual model explaining benthic foraminiferal microhabitats. Mar. Micropaleontol. 26, 3–15.
Jorissen, F.J., Fontanier, C., Thomas, E., 2007. Paleoceanographical proxies based on deep-sea benthic foraminiferal assemblage characteristics. In: Hillaire-Marcel, C., De Vernal, A. (Eds.), Proxies in Late Cenozoic Paleoceanography. Elsevier, Amsterdam, pp. 277–340.
Jost, L., 2006. Entropy and diversity. Oikos 113, 363–375.
Kaiser, H.F., 1960. The application of electronic computer to factor analysis. Educ. Psychol. Meas. 20, 141–151.
Kuhnt, T., Schmiedl, G., Ehrmann, W., Hamann, Y., Hemleben, C., 2007. Deep-sea ecosystem variability of the Aegean Sea during the past 22 kyr as revealed by benthic Foraminifera. Mar. Micropaleontol. 64, 141–162.
Lagaria, A., Mandalakis, M., Mara, P., Frangoulis, C., Karatsolis, B.-T., Pitta, P., Triantaphyllou, M., Tsiola, A., Psarra, S., 2017. Phytoplankton variability and community structure in relation to hydrographic features in the NE Aegean frontal area (NE Mediterranean Sea). Cont. Shelf Res. 149, 124–137.
Lampadariou, N., Tselepides, A., 2006. Spatial variability of meiofaunal communities at areas of contrasting depth and productivity in the Aegean Sea (NE Mediterranean). Prog. Oceanogr. 69, 19–36.
Lampadariou, N., Sevastou, K., Podaras, D., Tselepides, A., 2017. Insights into the benthic communities response to the inflow of Black Sea mesotrophic waters in the North Aegean Sea. Cont. Shelf Res. 149, 162–173.
Libes, S.M., Deuser, W.G., 1988. The isotope geochemistry of particulate nitrogen in the Peru upwelling area and the Gulf of Maine. Deep-Sea Res. Part I 35, 517–533.
Lirer, F., Sprovieri, M., Vallefuoco, M., Ferraro, L., Pelosi, N., Giordano, L., Capotondi, L., 2014. Planktonic foraminifera as bio-indicators for monitoring the climatic changes occurred during the last 2000 years in the SE Tyrrhenian Sea. Integr. Zool. 9, 542–554.
Loeblich, A.R., Tappan, H., 1987. Foraminiferal Genera and Their Classification, vol. 2. Van Nostrand Reinhold, New York.
Loeblich, A.R., Tappan, H., 1994. Foraminifera of the Sahul Shelf and Timor Sea. Cushman Foundation for Foraminiferal Research Special Publication, p. 31.
Luterbacher, J., García-Herrera, R., Akcer-On, S., Allan, R., Alvarez-Castro, M.C., Benito, G., Booth, J., Büntgen, U., Cagatay, N., Colombaroli, D., Davis, B., Esper, J., Felis, T., Fleitmann, D., Frank, D., Gallego, D., Garcia-Bustamante, E., Glaser, R., Gonzalez-Rouco, F.J., Goosse, H., Kiefer, T., Macklin, M.G., Manning, S.W., Montagna, P., Newman, L., Power, M.J., Rath, V., Ribera, P., Riemann, D., Roberts, N., Sicre, M.A., Silenzi, S., Tinner, W., Tzedakis, P., Valero-Garces, B., vander Schrier, G., Vanniere, B., Vogt, S., Wanner, H., Werner, J.P., Willett, G., Williams, M.H., Xoplaki, E., Zerefos, C.S., Zorita, E., 2012. A review of 2000 years of paleoclimatic evidence in the Mediterranean. In: Lionello, P. (Ed.), The Climate of the Mediterranean Region: from the Past to the Future. Elsevier, Amsterdam, pp. 87–185.
Luterbacher, J., Xoplaki, E., 2003. 500-Year winter temperature and precipitation variability over the mediterranean area and its connection to the large-scale atmospheric circulation. In: Bolle, H.-J. (Ed.), Mediterranean Climate. Variability and Trends. Springer Verlag, Berlin, pp. 133–153.
Lykousis, V., Chronis, G., Tselepides, A., Price, N.B., Theocharis, A., Siokou-Frangou, I., van Wambeke, F., Danovaro, R., Stavrakakis, S., Duineveld, G., Georgopoulos, L., Ignatiades, L., Souvermezoglou, A., Voutsinou-Taliadouri, F., 2002. Major outputs of the recent multidisciplinary biogeochemical researches undertaken in the Aegean Sea. J. Mar. Syst. 33–34, 313–334.
Malanotte-Rizzoli, P., Artale, V., Borzelli-Eusebi, G.L., Brenner, S., Civitarese, G., Crise, A., 2014. Physical forcing and physical/biochemical variability of the Mediterranean Sea: a review of unresolved issues and directions for future research. Ocean Sci. 10, 281–322.
Mann, M.E., Zhang, Z., Rutherford, S., Bradley, R.S., Hughes, M.K., Shindell, D., Ammann, C., Faluvegi, G., Ni, F., 2009. Global signatures and dynamical origins of the little ice age and medieval climate anomaly. Science 326, 1256–1260.
Margaritelli, G., Vallefuoco, M., Di Rita, F., Capotondi, L., Bellucci, L.G., Insinga, D.D., Petrosino, P., Bonomo, S., Cacho, I., Cascella, A., Ferraro, L., Florindo, F., Lubritto, C., Lurcock, P.C., Magri, D., Pelosi, N., Rettori, R., Lirer, F., 2016. Marine

response to climate changes during the last five millennia in the central Mediterranean Sea. Glob. Planet. Chang. 142, 53–72.
Mayewski, P.A., Meeker, L.D., Twickler, M.S., Whitlow, S., Yang, Q., Lyons, W.B., Prentice, M., 1997. Major features and forcing of high-latitude northern hemisphere atmospheric circulation using a 110,000-year long glaciochemical series. J. Geophys. Res. 102 (C12), 26345–26366.
Mayewski, P.A., Rohling, E.J., Stager, J.C., Karlen, W., Maasch, K.A., Meeker, L.D., Meyerson, E.A., Gasse, F., van Kreveld, S., Holmgren, K., Lee-Thorp, J., Rosqvist, G., Rack, F., Staubwasser, M., Schneider, R.R., Steig, E., 2004. Holocene climate variability. Quat. Res. 62, 243–255.
Menke, V., Ehrmann, W., Milker, Y., Brzelinski, S., Möbius, J., Mikolajewicz, U., Zolitschka, B., Zonneveld, K., Emeis, K.C., Schmiedl, G., 2017. Combined North Atlantic and anthropogenic forcing of changes in the marine environments in the Gulf of Taranto (Italy) during the last millennium. Climate of the Past Discussions. https://www.clim-pastdiscuss.net/cp-2017-139/.
Mercone, D., Thomson, J., Abu-Zied, R.H., Croudace, I.W., Rohling, E.J., 2001. High resolution geochemical and micropalaeontological profiling of the most recent eastern Mediterranean sapropel. Mar. Geol. 177, 25–44.
Meyers, P.A., 1994. Preservation of elemental and isotopic source identification of sedimentary organic matter. Chem. Geol. 114, 289–302.
Mojtahid, M., Jorissen, F., Lansard, B., Fontanier, C., Bombled, B., Rabouille, C., 2009. Spatial distribution of live benthic foraminifera in the Rhone prodelta: faunal response to a continental-marine organic matter gradient. Mar. Micropaleontol. 70, 177–200.
Morigi, C., Jorissen, F.J., Gervais, A., Guichard, S., Borsetti, A.M., 2001. Benthic foraminiferal faunas in surface sediments off NWAfrica: relationship with organic flux to the ocean floor. J. Foraminifer. Res. 31 (4), 350–368.
Nieto-Moreno, V., Martinez-Ruiz, F., Giralt, S., Gallego-Torres, D., García-Orellana, J., Masqué, P., Ortega-Huertas, M., 2013. Climate imprints during the'Medieval climate anomaly' and the 'little ice age' in marine records from the alboran Sea Basin. Holocene 23 (9), 1227–1237.
Nieto-Moreno, V., Martínez-Ruiz, F., Giralt, S., Jiménez-Espejo, F.J., Gallego-Torres, D., Rodrigo-Gàmiz, M., García-Orellana, J., Ortega-Huertas, M., de Lange, G.J., 2011. Tracking climate variability in the western Mediterranean during the Late Holocene: a multiproxy approach. Clim. Past 7, 1395–1414.
Ogrinc, N., Fontolan, G., Faganeli, J., Covelli, S., 2005. Carbon and nitrogen isotope compositions of organic matter in coastal marine sediments (the Gulf of Trieste, N Adriatic Sea): indicators of sources and preservation. Mar. Chem. 95, 163–181.
Ortega, P., Lehner, F., Swingedouw, D., Masson-Delmotte, D., Raible, C.C., Casado, M., Yiou, P., 2015. A model-tested North Atlantic Oscillation reconstruction for the past millennium. Nature 523, 71–74.
Parker, F.L., 1958. Eastern mediterranean foraminifera, sediment cores from the Mediterranean Sea, and the red sea. Reports of the Swedish Deep-Sea Expedition 8 (4), 219–285, 1947-1948.
Parker, W.C., Arnold, A.J., 1999. Quantitative methods of analysis in foraminiferal ecology. In: Sen Gupta, B.K. (Ed.), Modern Foraminifera. Kluwer Academic Publishers, Dordrecht, pp. 71–89.
Pierre, C., 1999. The oxygen and carbon isotope distribution in the Mediterranean water masses. Mar. Geol. 153, 41–55.
Piva, A., Asioli, A., Trincardi, F., Schneider, R.R., Vigliotti, L., 2008. Late-holocene climate variability in the Adriatic Sea (central mediterranean). Holocene 18, 153–167.
Poulos, S.E., 2009. Origin and distribution of the terrigenous component of the unconsolidated surface sediment of the Aegean floor: a synthesis. Cont. Shelf Res. 29, 2045–2060.
Poulos, S.E., Drakopoulos, P.G., Collins, M.B., 1997. Seasonal variability in sea surface oceanographic conditions in the Aegean Sea (eastern Mediterranean): an overview. J. Mar. Syst. 13, 225–244.
Reimer, P.J., Bard, E., Bayliss, A., Beck, J.W., Blackwell, P.G., Bronk Ramsey, C., Buck, C. E., Cheng, H., Edwards, R.L., Friedrich, M., 2013. IntCal13 and Marine13 radiocarbon age calibration curves 0-50,000 years cal BP. Radiocarbon 55, 1869–1887.
Reimer, P.J., McCormac, F.G., 2002. Marine radiocarbon reservoir corrections for the mediterranean and aegean seas. Radiocarbon 44, 159–166.
Roether, W., Manca, B.B., Klein, B., Bregant, D., Georgopoulos, D., Beitzel, V., Kovacevic, V., Luchetta, A., 1996. Recent changes in Eastern Mediterranean deep waters. Science 271, 333–335.
Rohling, E.J., Mayewski, P.A., Abu-Zied, R.H., Casford, J.S.L., Hayes, A., 2002. Holocene atmosphere-ocean interactions: records from Greenland and the Aegean. Clim. Dyn. 18, 587–593.
Rostek, F., Ruhland, G., Bassinot C., F., Mueller J., P., Labeyrie D., L., Lancelot, Y., Bard, E., 1993. Reconstructing sea surface temperature and salinity using $\delta^{18}O$ and alkenone records. Nature 364, 319–321.
Roussakis, G., Karageorgis, A.P., Conispoliatis, N., Lykousis, V., 2004. Last glacial-Holocene sediment sequences in N. Aegean basins: structure, accumulation rates and clay mineral distribution. Geo Mar. Lett. 24, 97–111.
Schilman, B., Bar-Matthews, M., Almogi-Labin, A., Luz, B., 2011. Global climate instability reflected by Eastern Mediterranean marine records during the late Holocene. Palaeogeogr. Palaeoclimatol. Palaeoecol. 176, 157–176.
Schmiedl, G., de Bovee, F., Buscail, R., Charriere, B., Hemleben, C., Medernach, L., Picon, P., 2000. Trophic control of benthic foraminiferal abundance and microhabitat in the bathyal Gulf of Lions, western Mediterranean Sea. Mar. Micropaleontol. 40, 167–188.
Schmiedl, G., Hemleben, C., Keller, J., Segl, M., 1998. Impact of climatic changes on the benthic foraminiferal fauna in the Ionian Sea during the last 330,000 years. Paleoceanography 13, 447–458.
Schmiedl, G., Kuhnt, T., Ehrmann, W., Emeis, K.-C., Hamann, Y., Kotthoff, U., Dulski, P., Pross, J., 2010. Climatic forcing of eastern Mediterranean deep-water formation and benthic ecosystems during the past 22 000 years. Quat. Sci. Rev. 29, 3006–3020.
Schmiedl, G., Mitschele, A., Beck, S., Emeis, K.-C., Hemleben, C., Schulz, H., Sperling, M., Weldeab, S., 2003. Benthic foraminiferal record of ecosystem variability in the eastern Mediterranean Sea during times of sapropel S5 and S6 deposition. Palaeogeogr. Palaeoclimatol. Palaeoecol. 190, 139–164.
Schweizer, M., 2006. Evolution and molecular phylogeny of cibicides and Uvigerina (rotaliida, foraminifera). Geol. Ultraiectina 261, 167.
Siani, G., Magny, M., Paterne, M., Debret, M., Fontugne, M., 2013. Paleohydrology reconstruction and holocene climate variability in the south adriatic sea. Clim. Past 9, 499–515.
Siokou-Frangou, I., Bianchi, M., Christaki, U., Christou, E.D., Giannakourou, A., Gotsis, O., Ignatiades, L., Pagou, K., Pitta, P., Psarra, S., Souvermezoglou, E., van Wambeke, F., Zervakis, V., 2002. Carbon flow in the planktonic food web along a gradient of oligotrophy in the Aegean Sea (Mediterranean Sea). J. Mar. Syst. 33–34, 335–353.
Shannon, C., Weaver, W., 1999. The Mathematical Theory of Communication, fifth ed. University of Illinois Press, p. 144.
Skampa, E., Triantaphyllou, M.V., Dimiza, M.D., Gogou, A., Malinverno, E., Stavrakakis, S., Panagiotopoulos, I.P., Parinos, C., Baumann, K.-H., 2019. Coupling plankton - sediment trap - surface sediment coccolithophore regime in the North Aegean Sea (NE Mediterranean). Mar. Micropaleontol. https://doi.org/10.1016/j.marmicro.2019.03.001.
Skliris, N., Sofianos, S., Gkanasos, A., Mantziafou, A., Vervatis, V., Axaopoulos, P., Lascaratos, A., 2012. Decadal scale variability of sea surface temperature in the Mediterranean Sea in relation to atmospheric variability. Ocean Dyn. 62, 13–30.
Souvermezoglou, E., Krasakopoulou, E., 2002. High oxygen consumption rates in the deep layers of the North Aegean Sea (eastern Mediterranean). Mediterr. Mar. Sci. 3, 55–64.
Sprovieri, M., Tranchida, G., Vallefuoco, M., Albertazzi, S., Bellucci, L.G., Bonanno, A., Bonomo, S., Censi, P., Ferraro, L., Giuliani, S., Mazzola, S., Sprovieri, R., 2010. The impact of the little ice age on coccolithophores in the central Mediterranean Sea. Clim. Past 6, 795–805.
Stothers, R.B., 1984. The great Tambora eruption in 1815 and its aftermath. Science 224, 1191–1198.
Theocharis, A., Georgopoulos, D., 1993. Dense water formation over the samothraki and Limnos plateaux in the North Aegean Sea (eastern Mediterranean Sea). Cont. Shelf Res. 13, 919–939.
Thornton, S.F., McManus, J., 1994. Application of organic carbon and nitrogen stable isotope and C/N ratios as source indicators of organic matter provenance in estuarine systems: evidence from the Tay Estuary, Scotland. Estuarine. Coastal and Shelf Science 38, 219–233.
Triantaphyllou, M.V., Gogou, A., Dimiza, M.D., Kostopoulou, S., Parinos, C., Roussakis, G., Geraga, M., Bouloubassi, I., Fleitmann, D., Zervakis, V., Velaoras, D., Diamantopoulou, A., Sampatakaki, A., Lykousis, V., 2016. Holocene climatic optimum centennial-scale paleoceanography in the NE Aegean (Mediterranean Sea). Geo Mar. Lett. 36, 51–66.
Tripsanas, E.K., Panagiotopoulos, I.P., Lykousis, V., Morfis, I., Karageorgis, A.P., Anastasakis, G., Kontogonis, G., 2016. Late quaternary bottom-current activity in the south Aegean Sea reflectinh climate-driven dense-water production. Mar. Geol. 375, 99–119.
Tsimplis, M.N., Rixen, M., 2002. Sea level in the Mediterranean Sea: the contribution of temperature and salinity changes. Geophys. Res. Lett. 29 (23), 2136.
Tyrlis, E., Lelieveld, J., Steil, B., 2012. The summer circulation over the eastern Mediterranean and the Middle East: influence of the South Asian monsoon. Clim. Dyn. 40, 1103–1123.
Velaoras, D., Kassis, D., Perivoliotis, L., Pagonis, P., Hondronasios, A., Nittis, K., 2013. Temperature and salinity variability in the Greek seas based on POSEIDON stations time series: preliminary results. Mediterr. Mar. Sci. 14, 5–18.
Velaoras, D., Lascaratos, A., 2005. Deep water mass characteristics and interannual variability in the North and Central Aegean Sea. J. Mar. Syst. 53, 59–85.
Velaoras, D., Lascaratos, A., 2010. North-Central Aegean Sea surface and intermediate water masses and their role in triggering the Eastern Mediterranean Transient. J. Mar. Syst. 83, 58–66.
Velaoras, D., Papadopoulos, V.P., Kontoyiannis, H., Papageorgiou, D., Pavlidou, A., 2017. The response of the Aegean Sea (eastern mediterranean) to the extreme 2016–2017 winter. Geophys. Res. Lett. 44 (18), 9416–9423.
Vervatis, V.D., Sofianos, S.S., Skliris, N., Somot, S., Lascaratos, A., Rixen, M., 2013. Mechanisms controlling the thermohaline circulation pattern variability in the Aegean-Levantine region. A hind cast simulation (1960-2000) with an eddy resolving model. Deep-Sea Res. Part I 74, 82–97.
Vogelsang, E., 1990. Palāo-Ozeanographie des Europäischen Nordmeeres an Hand stabiler Kohlenstoff- und Sauerstoff isotope. Berichte aus dem Sonderforsclumgsbercicli 313 (23), 1–136.
Wagner, S., Zorita, E., 2005. The influence of volcanic, solar and CO_2 forcing on the temperatures in the Dalton Minimum (1790–1830): a model study. Clim. Dyn. 25, 205–218.
WoRMS Editorial Board, 2018. World register of marine species. http://www.marinespecies.org/news.php?p=show&id=5395.
Zervakis, V., Georgopoulos, D., 1998. Hydrology and circulation in the north aegean (eastern mediterranean) throughout 1997 and 1998. Mediterr. Mar. Sci. 3, 7–21.
Zervakis, V., Georgopoulos, D., Drakopoulos, P.G., 2000. The role of the North Aegean in triggering the recent Eastern Mediterranean climatic changes. J. Geophys. Res. 105, 26103–26116.

Zervakis, V., Georgopoulos, D., Karageorgis, A.P., Theocharis, A., 2004. On the response of the Aegean Sea to climatic variability: a review. Int. J. Climatol. 24, 1845–1858.

Zervakis, V., Theocharis, A., Georgopoulos, D., 2005. Circulation and hydrography of the open seas. In: Papathanassiou, E., Zenetos, A. (Eds.), State of the Hellenic Marine Environment. HCMR Publications, Athens, pp. 104–110.

Zervoudaki, S., Christou, E.D., Nielsen, T.G., Siokou-Frangou, I., Assimakopoulou, G., Giannakourou, A., Maar, M., Pagou, K., Krasakopoulou, E., Christaki, U., Moraitou-Apostolopoulou, M., 2007. The importance of small size copepods in a frontal area of the Aegean Sea. J. Plankton Res. 29, 317–338.

Zodiatis, G., 1994. Advection of Black Sea water in the north Aegean Sea. Glob. Atmos. Ocean Syst. 2 (1), 41–60.